Coherent elastic neutrino-nucleus scattering on ^{40}Ar from first principles

C. G. Payne,[1] S. Bacca,[1] G. Hagen,[2, 3, *] W. Jiang,[3, 2] and T. Papenbrock[3, 2]

[1]*Institut für Kernphysik and PRISMA$^+$ Cluster of Excellence,*
Johannes Gutenberg-Universität, 55128 Mainz, Germany
[2]*Physics Division, Oak Ridge National Laboratory, Oak Ridge, TN 37831, USA*
[3]*Department of Physics and Astronomy, University of Tennessee, Knoxville, TN 37996, USA*

Coherent elastic neutrino scattering on the ^{40}Ar nucleus is computed with coupled-cluster theory based on nuclear Hamiltonians inspired by effective field theories of quantum chromodynamics. Our approach is validated by calculating the charge form factor and comparing it to data from electron scattering. We make predictions for the weak form factor, the neutron radius, and the neutron skin, and estimate systematic uncertainties. The neutron-skin thickness of ^{40}Ar is consistent with results from density functional theory. Precision measurements from coherent elastic neutrino-nucleus scattering could potentially be used to extract these observables and help to constrain nuclear models.

Introduction.–Fundamental properties of atomic nuclei, such as the distribution of the protons within the nucleus, are well determined from electron scattering experiments. In contrast, the distribution of the neutrons within the atomic nucleus, an equally important and fundamental property, is not as well known because it is difficult to measure. Parity violating electron scattering experiments [1–3] offer the least model dependent approach to experimentally probing the neutron distribution. Other processes occurring through neutral current weak interactions, i.e., by the exchange of a Z^0 boson, may offer an alternative and attractive opportunity in the future. A prominent example is coherent elastic neutrino-nucleus scattering (CEνNS), a process which is sensitive to the neutron distribution and the neutron radius [4–6]. Even though neutrinos are notoriously elusive particles, the COHERENT collaboration recently observed, for the first time, CEνNS from a sodium-doped CsI detector [7]. The experiment used stopped-pion neutrinos [8] from the Spallation Neutron Source at Oak Ridge National Laboratory, and discovered CEνNS at a 6.7σ confidence level with neutrinos coming from: delayed electron neutrinos, muon anti-neutrinos, and prompt muon neutrinos. The next stage of the COHERENT experiment is to switch to a ~ 1 ton target of liquid argon. Liquid argon will also be used in the future long-baseline neutrino experiment DUNE [9], which is aimed at extracting neutrino parameters from the observation of their oscillations. In addition, liquid argon is being used for a number of dark matter experiments (DEAP-3600 [10], DarkSide [11], ArDM [12], MiniCLEAN [13]), for which coherent neutrino scattering is important to determine the so-called neutrino floor. Studying the properties of the ^{40}Ar nucleus, the most abundant argon isotope composing the above mentioned detectors, is thus an important task for nuclear theory.

In the past decade we have seen an impressive progress in the theoretical and computational tools that underpin our understanding of the nucleus as a compound object of interacting protons and neutrons. A number of ab initio calculations of nuclear electroweak properties that start from interactions and currents obtained from chiral effective field theory have successfully described key observables, see, e.g., [14–18]. The level of accuracy and confidence reached by ab initio calculations in light- and medium-mass nuclei, along with the ability to access increasing mass numbers, allows us to address open questions in neutrino physics. This makes a first principles investigation of the ^{40}Ar nucleus both urgent and timely. For instance, neutrino elastic scattering has been discussed as a way to access the neutron-skin thickness [6], thus making it interesting to compute this quantity in ^{40}Ar. The neutron-skin thickness impacts the equation of state of infinite-nuclear matter and has astrophysical implications [19].

In this Letter we compute the nuclear weak form factor and the neutron-skin thickness with coupled-cluster theory from first principles, and provide theoretical predictions that may eventually be probed experimentally.

Coherent scattering.– Coherent elastic neutrino-nucleus scattering occurs in the regime $qR \ll 1$. Here $q = |\mathbf{q}|$ is the absolute value of the three-momentum transfer from the neutrino to the nucleus, and R is the weak nuclear radius. In this regime, the neutrino scatters coherently from the constituents of the nucleus, i.e., Z protons and N neutrons. The CEνNS cross section is

$$\frac{d\sigma}{dT}(E_\nu, T) \simeq \frac{G_F^2}{4\pi} M \left[1 - \frac{MT}{2E_\nu^2}\right] Q_W^2 F_W^2(q^2). \quad (1)$$

Here G_F is the Fermi constant, M is the mass of the nucleus, E_ν is the energy of the neutrino beam, and T is the nuclear recoil energy. The weak charge Q_W and weak form factor $F_W(q^2)$ are defined as

$$Q_W = N - (1 - 4\sin^2\theta_W)Z \,, \qquad (2)$$

$$F_W(q^2) = \frac{1}{Q_W}\left[NF_n(q^2) - (1 - 4\sin^2\theta_W)ZF_p(q^2)\right] \,,$$

respectively. Here θ_W is the Weinberg weak mixing angle, and $F_{n,p}(q^2)$ is the proton (p) and neutron (n) form factor, respectively. Using the low-energy value of θ_W [20] from the Particle Data Group, one obtains $1 - 4\sin^2\theta_W(0) = 0.0457 \pm 0.0002$. Thus, the weak form factor becomes $F_W(q^2) \simeq F_n(q^2)$, and CEνNS is mainly sensitive to the distribution of neutrons within the nucleus. The resulting cross section scales as N^2. In this paper we will consider low-q ranges and investigate effects due to the nuclear structure. For ^{40}Ar, the coherence condition limits $q \lesssim 50$ MeV/c, but we are also interested in exploring the form factors as ground-state observables in a wider momentum range.

Method.– Our computations are based on coupled cluster theory [21–29], where one solves the Schrödinger equation

$$\overline{H}_N|\Phi_0\rangle = E|\Phi_0\rangle \qquad (3)$$

based on the reference state $|\Phi_0\rangle$ of a closed-shell nucleus. The similarity transformed Hamiltonian is

$$\overline{H}_N = e^{-T}H_N e^T \,. \qquad (4)$$

The Hamiltonian $\overline{H}_N$ is normal-ordered with respect to the reference state. The operator $T = T_1 + T_2 + T_3 + \ldots$ is expanded in particle-hole excitations with respect to the reference and is truncated at some low-rank particle-hole excitation level. Following Ref. [30], we will denote coupled-cluster singles and doubles calculations (where $T = T_1 + T_2$) with "D", while calculations that include linearized triples will be labeled with "T-1"; we refer the reader to that paper and the review [29] for details on the accuracy of various coupled-cluster approximations in nuclei.

The open-shell nucleus ^{40}Ar has $Z = 18$ protons and $N = 22$ neutrons. We calculate its ground state using a double-charge-exchange equation-of-motion technique [31] starting from the closed-shell nucleus ^{40}Ca. This technique is a generalization of single-charge exchange, used previously to describe the daughter nuclei resulting from β-decays of closed-shell nuclei such as ^{14}C [32] and ^{100}Sn [17]. The double-charge-exchange operator

$$R = \frac{1}{4}\sum_{p,p',n,n'} r^{nn'}_{pp'}\hat{n}^\dagger \hat{n'}^\dagger \hat{p'}\hat{p}$$

$$+ \frac{1}{36}\sum_{N,N',p,p',n,n'} r^{Nnn'}_{N'pp'}\hat{n}^\dagger \hat{n'}^\dagger \hat{N}^\dagger \hat{N'}\hat{p'}\hat{p} \qquad (5)$$

generates the ground-state of ^{40}Ar as an excitation of the ^{40}Ca. Here, $\hat{p}$, $\hat{n}$, and $\hat{N}$ annihilate a proton, neutron, and nucleon, respectively. The excitation amplitudes $r^{nn'}_{pp'}$ and $r^{Nnn'}_{N'pp'}$ are solutions of the eigenvalue problem $\overline{H}_N R = ER$, and the lowest eigenvalue E is the ground-state energy of ^{40}Ar. Likewise, we define a left excitation operator L and also solve $L\overline{H}_N = EL$ (because $\overline{H}_N$ is not Hermitian). This allows us to evaluate ground-state expectation values (such as the density) of operators $\hat{O}$ as $\langle L|\overline{O}|R\rangle$. Here, $\overline{O}$ is the similarity transform of the operator $\hat{O}$.

The computations shown in this work are based on a model space that includes 15 major shells (unless otherwise specified) and an harmonic oscillator parameter $\hbar\Omega = 16$ MeV. When we include leading triples T-1, we use an energy truncation $E_{3\text{max}}$ cut at 18 oscillator spacings, where we reach a sub-percentage convergence of the form factors in the considered momentum range.
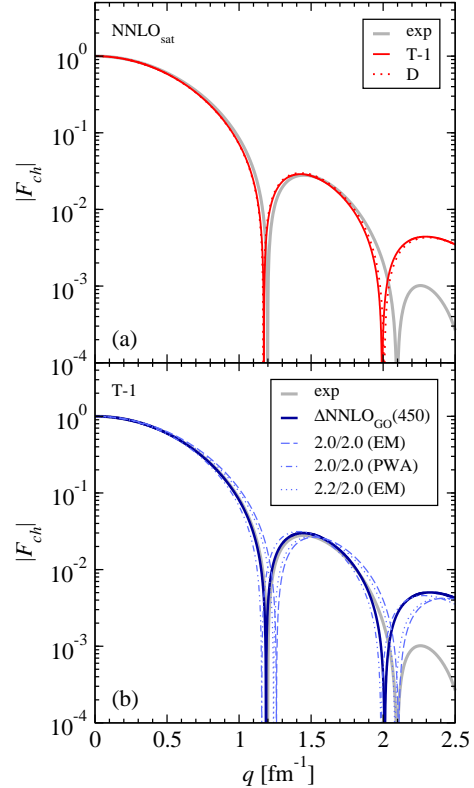

FIG. 1. Panel (a): ^{40}Ar charge form factor computed with the NNLO$_{\text{sat}}$ interaction at two different levels of correlations (D and T-1), compared to experimental data (exp) by Ottermann *et al.* [33]. Panel (b): ^{40}Ar charge form factor computed with various different interactions at the T-1 level, also compared to the experimental data. See text for more details.

Interactions.– We employ Hamiltonians from chiral effective field theories (χ-EFT) of quantum chromodynamics (QCD) [34–36]. In this framework, Hamiltonians are

expressed in terms of nucleons and pions and are consistent with the symmetries and broken chiral symmetry of QCD. They are expanded in powers of $(Q/\Lambda_\chi)^\nu$, where Q is the low-momentum scale characterizing nuclear physics, and $\Lambda_\chi \sim 1$ GeV is the QCD scale. The coefficients of the Hamiltonian expansion are low-energy constants (LECs); they encapsulate the unresolved short-range physics and are typically calibrated by adjusting theoretical results to experimental data. The accuracy of a calculation is controlled by the order ν of the employed dynamical ingredients and by the accuracy to which one can solve the many-body problem. In this work we implement Hamiltonians derived at next-to-next-to-leading order or higher ($\nu = 3$ or 4). To probe the systematic uncertainties, we employ various chiral potentials. In particular, we use the $NNLO_{sat}$ interaction [37], for which the LECs entering the two-body and three-body forces are adjusted to nucleon-nucleon phase shifts and to energies and charge radii of light nuclei up to ^{24}O. We also use the $\Delta NNLO_{GO}(450)$ potential [38], a delta-full χ-EFT interaction at next-to-next-to-leading order [39], which was adjusted to light nuclei, and the saturation point and symmetry energy of nuclear matter. Finally, we employ selected soft potentials obtained by performing a similarity renormalization group transformation [40] of the two-body chiral potential by Entem and Machleidt [41], with leading-order three-nucleon forces from χ-EFT adjusted to the binding energy of ^3H and the charge radius of ^4He [42, 43]. For these interactions we follow the notation of Ref. [43], namely 1.8/2.0, 2.0/2.0, 2.2/2.0 (EM) and 2.0/2.0 (PWA), where the first (second) number indicates the cutoff of the two-body (three-body) force in fm^{-1}, and EM indicates that the pion-nucleon LECs entering the three-nucleon force are taken from the Entem and Machleidt potential [41], while in PWA they are taken from partial wave analysis data. For electroweak operators we take the one-body terms, as two-body currents are expected to be negligible [44, 45], especially so at the low momenta of CEνNS.

Results. – Figure 1 shows our results for the ^{40}Ar charge form factor F_{ch} as a function of q, and compares them to electron-scattering data from Ottermann *et al.* [33]. This comparison validates the theory. Panel (a) shows results from the $NNLO_{sat}$ interaction for different correlation levels of the coupled-cluster expansion. We see that increasing the correlations from D to T-1 changes the form factor only slightly, and the results are sufficiently well converged. This is consistent with results from previous studies [30, 48], where triples correlations only affected the radii below 1%. Panel (b) shows calculations of the charge form factor at the T-1 level for different interactions. As representative examples we chose the 2.0/2.0 (EM), 2.0/2.0 (PWA), and 2.2/2.0 (EM) potentials. The form factors exhibit a dependence on the choice of the Hamiltonian, particularly at larger momentum transfers. The interaction $\Delta NNLO_{GO}(450)$,
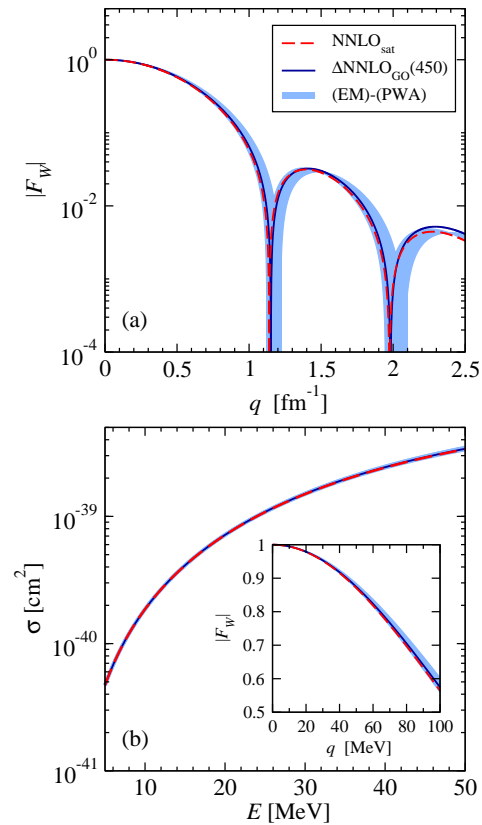

FIG. 2. Panel (a): ^{40}Ar weak form factor computed with different Hamiltonians. The EM-family interactions are shown as a band. Panel (b): CEνNS as a function of the neutrino energy, computed with same three different Hamiltonians. The inset shows the form factor zoomed into the low-q region relevant to coherent scattering, in linear scale.

derived in a delta-full chiral framework, provides a qualitatively similar description of the experimental data as the $NNLO_{sat}$, noting that the former interaction reproduces the first minimum of $|F_{ch}|$ more precisely. We remind the reader that – within the Helm model [49] – the first zero of the form factor is proportional to the inverse radius of the charge distribution. Among the family of EM potentials, the 2.2/2.0 (EM) interactions predicts the first zero at higher q, consistent with a smaller charge radius. Overall, one should trust the Hamiltonians only for momentum transfers up to about $q = 2.0$ fm^{-1}, which marks the scale of the employed ultraviolet cutoffs.

Figure 2(a) shows the ^{40}Ar weak form factor F_W of Eq. (2) as a function of the momentum transfer q, calculated in the T-1 scheme. Here, we show the soft interactions with a band that encompasses the three different potentials, labeled with (EM)-(PWA). The weak form factor exhibits a mild dependence on the choice of the Hamiltonian. The band spanned by the from factors of the EM interactions exhibits a first dip at a larger q value than the potentials $NNLO_{sat}$ and the $\Delta NNLO_{GO}(450)$,
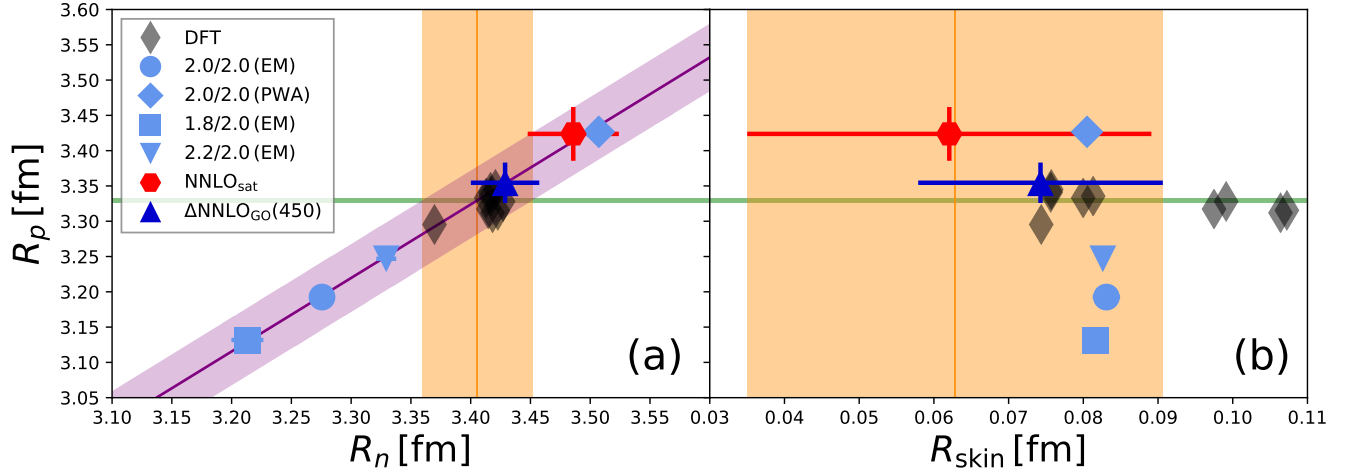
FIG. 3. Correlation between R_p and R_n (a) and between R_p and $R_{\rm skin}$ (b) for various Hamiltonians. The experimental R_p is also shown by the horizontal green line [46], as well as the DFT data [47] by the diamonds.

which are very similar. Our results are consistent with a Helm form factor parameterized by a box radius of 3.83 fm and a surface thickness of 0.9 fm [6]. We also note that our ab initio results for the weak form factor agree with calculations from density functional theory [5].

Let us consider the CEνNS cross section. Figure 2(b) shows the cross section calculated from Eq. (1) via $q^2 = 2E_\nu MT/(E_\nu - T) \approx 2MT$, as a function of the neutrino beam energy, for three different interactions. The results are virtually independent of the employed potential, because only the low-momentum part of the weak form factor contributes to the cross section. The inset of Fig. 2(b) shows the weak form factor for momentum transfers relevant to the coherent elastic neutrino-nucleus scattering. Even on the shown linear scale, one observes only a mild nuclear-structure dependence. For example, at $q = 50$ and 100 MeV, F_W has a 2% and 6% spread, respectively. Consequently, CEνNS is required to reach a high precision in order to probe differences in nuclear Hamiltonians. We remind the reader that the CEνNS signal scales with N^2, possibly making heavier nuclei such as caesium or iodine more attractive detector materials for this purpose than ^{40}Ar.

Overall, the weak form factor has a very similar shape to the charge form factor. For the NNLO$_{\rm sat}$ interaction, at $q = 0.25$ fm^{-1} (1 fm^{-1}) F_W is 0.5% (20%) smaller than F_{ch}, while the first dip of F_W falls about 0.035 fm^{-1} earlier than that of F_{ch}, meaning the neutron distribution extends further out from that of the protons.

We now turn to the computation of the point-proton R_p and point-neutron R_n radii for ^{40}Ar, as well as its neutron-skin thickness, defined as $R_{\rm skin} = R_n - R_p$. Figure 3 shows the results obtained with T-1 coupled-cluster calculations for six different potentials. We employ the five previous ones and one other member of the EM-interaction family [43], namely the 1.8/2.0 (EM)

interaction. The uncertainties of R_p and R_n are the difference between a T-1 and a D coupled-cluster theory calculation, and we take the maximum of the two values as the uncertainty for both. Our model space consists of 15 oscillator shells, except for the softest 1.8/2.0 (EM), which was already converged in 11 shells. As expected, uncertainties are larger for the harder interactions NNLO$_{\rm sat}$ and ΔNNLO$_{\rm GO}$(450).

As previously reported for ^{48}Ca [50], Fig. 3(a) also shows a strong correlation between $R_{\rm p}$ and $R_{\rm n}$. We would like to remark that this is a non-trivial correlation: in the EM-family interactions we vary the cutoff in the two-body force while the LECs in the three-nucleon force are different; furthermore, by employing the NNLO$_{\rm sat}$ and ΔNNLO$_{\rm GO}$(450) potentials we also explore different cutoffs in the three-body force. The spread of the radii due to the variation of the employed Hamiltonians is about 10%. As in Ref. [50], a narrower constraint can be provided by intersecting the correlation band – obtained by linearly joining all our calculations with a symmetric spread (in purple) given by the maximum uncertainty bar – with the experimental value on R_p taken from [46]. This yields $3.36 \leq R_n \leq 3.45$ fm. Results from density functional theory [5, 47] are shown as the diamonds in Fig. 3(a). These are all clustered around our constraint for R_n. Within uncertainties, our charge radius is also consistent with the recent ab initio computations of Ref. [18].

Results for the neutron skin are shown in Fig. 3(b). Because the neutron and proton radii are strongly correlated, the variation in $R_{\rm skin}$ is much reduced. The uncertainty of $R_{\rm skin}$ is the difference between the T-1 and D coupled-cluster computations. We predict the neutron-skin thickness of ^{40}Ar in the range $0.035 - 0.09$ fm. The results from density functional theory [5, 47] are again shown as diamonds. While consistent with the ab ini-

tio computation, we see that density functional theory predicts a slightly larger neutron-skin thickness.

Summary.– We performed calculations of the ^{40}Ar charge and weak form factors and observed a dependence on the choice of the employed Hamiltonian, which is mild at low-q and moderate in the region of the first diffraction minimum. This fact is important, because it suggests that nuclear physics uncertainties will likely not limit the sensitivity to new physics [51]. From the weak form factor, we calculated the coherent elastic neutrino-nucleus scattering and observed that the Hamiltonian dependence is probably too small to be disentangled by the COHERENT experiment. On the other hand, we also provide predictions for the neutron-, proton-, and neutron-skin thickness by exploiting the correlations of coupled-cluster computations with various Hamiltonians with the experimental value of R_p. The computed R_n and R_{skin} of ^{40}Ar are consistent with results from density functional theory, and CEνNS with much improved precision could help to constrain Hamiltonians from χ-EFT.

[1] S. Abrahamyan, Z. Ahmed, H. Albataineh, K. Aniol, D. S. Armstrong, W. Armstrong, T. Averett, B. Babineau, A. Barbieri, V. Bellini, R. Beminiwattha, J. Benesch, F. Benmokhtar, T. Bielarski, W. Boeglin, A. Camsonne, M. Canan, P. Carter, G. D. Cates, C. Chen, J.-P. Chen, O. Hen, F. Cusanno, M. M. Dalton, R. De Leo, K. de Jager, W. Deconinck, P. Decowski, X. Deng, A. Deur, D. Dutta, A. Etile, D. Flay, G. B. Franklin, M. Friend, S. Frullani, E. Fuchey, F. Garibaldi, E. Gasser, R. Gilman, A. Giusa, A. Glamazdin, J. Gomez, J. Grames, C. Gu, O. Hansen, J. Hansknecht, D. W. Higinbotham, R. S. Holmes, T. Holmstrom, C. J. Horowitz, J. Hoskins, J. Huang, C. E. Hyde, F. Itard, C.-M. Jen, E. Jensen, G. Jin, S. Johnston, A. Kelleher, K. Kliakhandler, P. M. King, S. Kowalski, K. S. Kumar, J. Leacock, J. Leckey, J. H. Lee, J. J. LeRose, R. Lindgren, N. Liyanage, N. Lubinsky, J. Mammei, F. Mammoliti, D. J. Margaziotis, P. Markowitz, A. McCreary, D. McNulty, L. Mercado, Z.-E. Meziani, R. W. Michaels, M. Mihovilovic, N. Muangma, C. Muñoz Camacho, S. Nanda, V. Nelyubin, N. Nuruzzaman, Y. Oh, A. Palmer, D. Parno, K. D. Paschke, S. K. Phillips, B. Poelker, R. Pomatsalyuk, M. Posik, A. J. R. Puckett, B. Quinn, A. Rakhman, P. E. Reimer, S. Riordan, P. Rogan, G. Ron, G. Russo, K. Saenboonruang, A. Saha, B. Sawatzky, A. Shahinyan, R. Silwal, S. Sirca, K. Slifer, P. Solvignon, P. A. Souder, M. L. Sperduto, R. Subedi, R. Suleiman, V. Sulkosky, C. M. Sutera, W. A. Tobias, W. Troth, G. M. Urciuoli, B. Waidyawansa, D. Wang, J. Wexler, R. Wilson, B. Wojtsekhowski, X. Yan, H. Yao, Y. Ye, Z. Ye, V. Yim, L. Zana, X. Zhan, J. Zhang, Y. Zhang, X. Zheng, and P. Zhu (PREX Collaboration), "Measurement of the neutron radius of ^{208}Pb through parity violation in electron scattering," Phys. Rev. Lett. **108**, 112502 (2012).

[2] C. J. Horowitz, K. S. Kumar, and R. Michaels, "Electroweak Measurements of Neutron Densities in CREX and PREX at JLab, USA," Eur. Phys. J. **A50**, 48 (2014), arXiv:1307.3572 [nucl-ex].

[3] M. Thiel, C. Sfienti, J. Piekarewicz, C.J. Horowitz, and Vanderhaeghen. M., "Neutron skins of atomic nuclei: per aspera ad astra," Journal of Physics G: Nuclear and Particle Physics **46**, 093003 (2019).

[4] P. S. Amanik and G. C. McLaughlin, "Nuclear neutron form factor from neutrino–nucleus coherent elastic scattering," Journal of Physics G: Nuclear and Particle Physics **36**, 015105 (2009).

[5] K. Patton, J. Engel, G. C. McLaughlin, and N. Schunck, "Neutrino-nucleus coherent scattering as a probe of neutron density distributions," Phys. Rev. C **86**, 024612 (2012).

[6] M. Cadeddu, C. Giunti, Y. F. Li, and Y. Y. Zhang, "Average CsI neutron density distribution from coherent data," Phys. Rev. Lett. **120**, 072501 (2018).

[7] D. Akimov, J. B. Albert, P. An, C. Awe, P. S. Barbeau, B. Becker, V. Belov, A. Brown, A. Bolozdynya, B. Cabrera-Palmer, M. Cervantes, J. I. Collar, R. J. Cooper, R. L. Cooper, C. Cuesta, D. J. Dean, J. A. Detwiler, A. Eberhardt, Y. Efremenko, S. R. Elliott, E. M. Erkela, L. Fabris, M. Febbraro, N. E. Fields, W. Fox, Z. Fu, A. Galindo-Uribarri, M. P. Green, M. Hai, M. R. Heath, S. Hedges, D. Hornback, T. W. Hossbach, E. B. Iverson, L. J. Kaufman, S. Ki, S. R. Klein, A. Khromov, A. Konovalov, M. Kremer, A. Kumpan, C. Leadbetter, L. Li, W. Lu, K. Mann, D. M. Markoff, K. Miller, H. Moreno, P. E. Mueller, J. Newby, J. L. Orrell, C. T. Overman, D. S. Parno, S. Penttila, G. Perumpilly, H. Ray, J. Raybern, D. Reyna, G. C. Rich, D. Rimal, D. Rudik, K. Scholberg, B. J. Scholz, G. Sinev, W. M. Snow, V. Sosnovtsev, A. Shakirov, S. Suchyta, B. Suh, R. Tayloe, R. T. Thornton, I. Tolstukhin, J. Vanderwerp, R. L. Varner, C. J. Virtue, Z. Wan, J. Yoo, C.-H. Yu, A. Zawada, J. Zettlemoyer, and A. M. Zderic, "Observation of coherent elastic neutrino-nucleus scattering," Science **357**, 1123–1126 (2017), http://science.sciencemag.org/content/357/6356/1123.full.pdf.

[8] K. Scholberg, "Prospects for measuring coherent neutrino-nucleus elastic scattering at a stopped-pion neutrino source," Phys. Rev. D **73**, 033005 (2006).

[9] "Deep underground neutrino experiment," http://www.dunescience.org.

[10] "Deap," DEAP-3600: deap3600.ca.

[11] "Darkside," http://darkside.lngs.infn.it/.

[12] "Ardm," http://darkmatter.ethz.ch/.

[13] "Miniclean," Mini Clean : http://deapclean.org/.

[14] S. Bacca and S. Pastore, "Electromagnetic reactions on light nuclei," Journal of Physics G: Nuclear and Particle Physics **41**, 123002 (2014).

[15] A. Lovato, S. Gandolfi, J. Carlson, Steven C. Pieper, and R. Schiavilla, "Neutral weak current two-body contributions in inclusive scattering from ^{12}C," Phys. Rev. Lett. **112**, 182502 (2014).

[16] S. Pastore, A. Baroni, J. Carlson, S. Gandolfi, Steven C. Pieper, R. Schiavilla, and R. B. Wiringa, "Quantum Monte Carlo calculations of weak transitions in $A = 6 - 10$ nuclei," Phys. Rev. C **97**, 022501 (2018).

[17] P. Gysbers, G. Hagen, J. D. Holt, G. R. Jansen, T. D. Morris, P. Navrátil, T. Papenbrock, S. Quaglioni, A. Schwenk, S. R. Stroberg, and K. A. Wendt, "Discrepancy between experimental and theoretical β-decay rates resolved from first principles," Nature Physics **15**, 428–431 (2019).

[18] C. Barbieri, N. Rocco, and V. Somà, "Lepton scattering from ^{40}Ar and Ti in the quasielastic peak region," (2019), arXiv:1907.01122 [nucl-th].

[19] J. M. Lattimer, "The nuclear equation of state and neutron star masses," Annual Review of Nuclear and Particle Science **62**, 485–515 (2012), https://doi.org/10.1146/annurev-nucl-102711-095018.

[20] M. Tanabashi, K. Hagiwara, K. Hikasa, K. Nakamura, Y. Sumino, F. Takahashi, J. Tanaka, K. Agashe, G. Aielli, C. Amsler, M. Antonelli, D. M. Asner, H. Baer, Sw. Banerjee, R. M. Barnett, T. Basaglia, C. W. Bauer, J. J. Beatty, V. I. Belousov, J. Beringer, S. Bethke, A. Bettini, H. Bichsel, O. Biebel, K. M. Black, E. Blucher, O. Buchmuller, V. Burkert, M. A. Bychkov, R. N. Cahn, M. Carena, A. Ceccucci, A. Cerri, D. Chakraborty, M.-C. Chen, R. S. Chivukula, G. Cowan, O. Dahl, G. D'Ambrosio, T. Damour, D. de Florian, A. de Gouvêa, T. DeGrand, P. de Jong, G. Dissertori, B. A. Dobrescu, M. D'Onofrio, M. Doser, M. Drees, H. K. Dreiner, D. A. Dwyer, P. Eerola, S. Eidelman, J. Ellis, J. Erler, V. V. Ezhela, W. Fetscher, B. D. Fields, R. Firestone, B. Foster, A. Freitas, H. Gallagher, L. Garren, H.-J. Gerber, G. Gerbier, T. Gershon, Y. Gershtein, T. Gherghetta, A. A. Godizov, M. Goodman, C. Grab, A. V. Gritsan, C. Grojean, D. E. Groom, M. Grünewald, A. Gurtu, T. Gutsche, H. E. Haber, C. Hanhart, S. Hashimoto, Y. Hayato, K. G. Hayes, A. Hebecker, S. Heinemeyer, B. Heltsley, J. J. Hernández-Rey, J. Hisano, A. Höcker, J. Holder, A. Holtkamp, T. Hyodo, K. D. Irwin, K. F. Johnson, M. Kado, M. Karliner, U. F. Katz, S. R. Klein, E. Klempt, R. V. Kowalewski, F. Krauss, M. Kreps, B. Krusche, Yu. V. Kuyanov, Y. Kwon, O. Lahav, J. Laiho, J. Lesgourgues, A. Liddle, Z. Ligeti, C.-J. Lin, C. Lippmann, T. M. Liss, L. Littenberg, K. S. Lugovsky, S. B. Lugovsky, A. Lusiani, Y. Makida, F. Maltoni, T. Mannel, A. V. Manohar, W. J. Marciano, A. D. Martin, A. Masoni, J. Matthews, U.-G. Meißner, D. Milstead, R. E. Mitchell, K. Mönig, P. Molaro, F. Moortgat, M. Moskovic, H. Murayama, M. Narain, P. Nason, S. Navas, M. Neubert, P. Nevski, Y. Nir, K. A. Olive, S. Pagan Griso, J. Par-

sons, C. Patrignani, J. A. Peacock, M. Pennington, S. T. Petcov, V. A. Petrov, E. Pianori, A. Piepke, A. Pomarol, A. Quadt, J. Rademacker, G. Raffelt, B. N. Ratcliff, P. Richardson, A. Ringwald, S. Roesler, S. Rolli, A. Romaniouk, L. J. Rosenberg, J. L. Rosner, G. Rybka, R. A. Ryutin, C. T. Sachrajda, Y. Sakai, G. P. Salam, S. Sarkar, F. Sauli, O. Schneider, K. Scholberg, A. J. Schwartz, D. Scott, V. Sharma, S. R. Sharpe, T. Shutt, M. Silari, T. Sjöstrand, P. Skands, T. Skwarnicki, J. G. Smith, G. F. Smoot, S. Spanier, H. Spieler, C. Spiering, A. Stahl, S. L. Stone, T. Sumiyoshi, M. J. Syphers, K. Terashi, J. Terning, U. Thoma, R. S. Thorne, L. Tiator, M. Titov, N. P. Tkachenko, N. A. Törnqvist, D. R. Tovey, G. Valencia, R. Van de Water, N. Varelas, G. Venanzoni, L. Verde, M. G. Vincter, P. Vogel, A. Vogt, S. P. Wakely, W. Walkowiak, C. W. Walter, D. Wands, D. R. Ward, M. O. Wascko, G. Weiglein, D. H. Weinberg, E. J. Weinberg, M. White, L. R. Wiencke, S. Willocq, C. G. Wohl, J. Womersley, C. L. Woody, R. L. Workman, W.-M. Yao, G. P. Zeller, O. V. Zenin, R.-Y. Zhu, S.-L. Zhu, F. Zimmermann, P. A. Zyla, J. Anderson, L. Fuller, V. S. Lugovsky, and P. Schaffner (Particle Data Group), "Review of particle physics," Phys. Rev. D **98**, 030001 (2018).

[21] F. Coester, "Bound states of a many-particle system," Nuclear Physics **7**, 421 – 424 (1958).

[22] F. Coester and H. Kümmel, "Short-range correlations in nuclear wave functions," Nuclear Physics **17**, 477 – 485 (1960).

[23] H. Kümmel, K. H. Lührmann, and J. G. Zabolitzky, "Many-fermion theory in expS- (or coupled cluster) form," Physics Reports **36**, 1 – 63 (1978).

[24] R. F. Bishop, "An overview of coupled cluster theory and its applications in physics," Theoretical Chemistry Accounts: Theory, Computation, and Modeling (Theoretica Chimica Acta) **80**, 95–148 (1991).

[25] B. Mihaila and J. H. Heisenberg, "Microscopic Calculation of the Inclusive Electron Scattering Structure Function in ^{16}O," Phys. Rev. Lett. **84**, 1403–1406 (2000).

[26] D. J. Dean and M. Hjorth-Jensen, "Coupled-cluster approach to nuclear physics," Phys. Rev. C **69**, 054320 (2004).

[27] K. Kowalski, D. J. Dean, M. Hjorth-Jensen, T. Papenbrock, and P. Piecuch, "Coupled cluster calculations of ground and excited states of nuclei," Phys. Rev. Lett. **92**, 132501 (2004).

[28] R. J. Bartlett and M. Musiał, "Coupled-cluster theory in quantum chemistry," Rev. Mod. Phys. **79**, 291–352 (2007).

[29] G. Hagen, T. Papenbrock, M. Hjorth-Jensen, and D. J. Dean, "Coupled-cluster computations of atomic nuclei," Rep. Prog. Phys. **77**, 096302 (2014).

[30] M. Miorelli, S. Bacca, G. Hagen, and T. Papenbrock, "Computing the dipole polarizability of ^{48}Ca with increased precision," Phys. Rev. C **98**, 014324 (2018).

[31] H. N. Liu, A. Obertelli, P. Doornenbal, C. A. Bertulani, G. Hagen, J. D. Holt, G. R. Jansen, T. D. Morris, A. Schwenk, R. Stroberg, N. Achouri, H. Baba, F. Browne, D. Calvet, F. Château, S. Chen, N. Chiga, A. Corsi, M. L. Cortés, A. Delbart, J.-M. Gheller, A. Giganon, A. Gillibert, C. Hilaire, T. Isobe, T. Kobayashi, Y. Kubota, V. Lapoux, T. Motobayashi, I. Murray, H. Otsu, V. Panin, N. Paul, W. Rodriguez, H. Sakurai, M. Sasano, D. Steppenbeck, L. Stuhl, Y. L. Sun, Y. Togano, T. Uesaka, K. Wimmer, K. Yoneda,

O. Aktas, T. Aumann, L. X. Chung, F. Flavigny, S. Franchoo, I. Gašparić, R.-B. Gerst, J. Gibelin, K. I. Hahn, D. Kim, T. Koiwai, Y. Kondo, P. Koseoglou, J. Lee, C. Lehr, B. D. Linh, T. Lokotko, M. MacCormick, K. Moschner, T. Nakamura, S. Y. Park, D. Rossi, E. Sahin, D. Sohler, P.-A. Söderström, S. Takeuchi, H. Törnqvist, V. Vaquero, V. Wagner, S. Wang, V. Werner, X. Xu, H. Yamada, D. Yan, Z. Yang, M. Yasuda, and L. Zanetti, "How robust is the $n = 34$ subshell closure? first spectroscopy of ^{52}Ar," Phys. Rev. Lett. **122**, 072502 (2019).

[32] A. Ekström, G. R. Jansen, K. A. Wendt, G. Hagen, T. Papenbrock, S. Bacca, B. Carlsson, and D. Gazit, "Effects of Three-Nucleon Forces and Two-Body Currents on Gamow-Teller Strengths," Phys. Rev. Lett. **113**, 262504 (2014).

[33] C.R. Ottermann, C.H. Schmitt, G.G. Simon, F. Borkowski, and V.H. Walther, "Elastic electron scattering from 40ar," Nuclear Physics A **379**, 396 – 406 (1982).

[34] U. Van Kolck, "Effective field theory of nuclear forces," Prog. Part. Nucl. Phys. **43**, 337 – 418 (1999).

[35] E. Epelbaum, H.-W. Hammer, and Ulf-G. Meißner, "Modern theory of nuclear forces," Rev. Mod. Phys. **81**, 1773–1825 (2009).

[36] R. Machleidt and D.R. Entem, "Chiral effective field theory and nuclear forces," Physics Reports **503**, 1 – 75 (2011).

[37] A. Ekström, B. D. Carlsson, K. A. Wendt, C. Forssén, M. Hjorth Jensen, R. Machleidt, and S. M. Wild, "Statistical uncertainties of a chiral interaction at next-to-next-to leading order," J. Phys, G: Nucl. Part. Phys. **42**, 034003 (2015).

[38] W. Jiang *et al.*, in preparation.

[39] A. Ekström, G. Hagen, T. D. Morris, T. Papenbrock, and P. D. Schwartz, "Δ isobars and nuclear saturation," Phys. Rev. C **97**, 024332 (2018).

[40] S. K. Bogner, R. J. Furnstahl, and R. J. Perry, "Similarity renormalization group for nucleon-nucleon interactions," Phys. Rev. C **75**, 061001 (2007).

[41] D. R. Entem and R. Machleidt, "Accurate charge-dependent nucleon-nucleon potential at fourth order of chiral perturbation theory," Phys. Rev. C **68**, 041001 (2003).

[42] A. Nogga, S. K. Bogner, and A. Schwenk, "Low-momentum interaction in few-nucleon systems," Phys. Rev. C **70**, 061002 (2004).

[43] K. Hebeler, S. K. Bogner, R. J. Furnstahl, A. Nogga, and A. Schwenk, "Improved nuclear matter calculations from chiral low-momentum interactions," Phys. Rev. C **83**, 031301 (2011).

[44] A. Lovato, S. Gandolfi, Ralph Butler, J. Carlson, Ewing Lusk, Steven C. Pieper, and R. Schiavilla, "Charge form factor and sum rules of electromagnetic response functions in ^{12}C," Phys. Rev. Lett. **111**, 092501 (2013).

[45] M. Piarulli, L. Girlanda, L. E. Marcucci, S. Pastore, R. Schiavilla, and M. Viviani, "Electromagnetic structure of $a = 2$ and 3 nuclei in chiral effective field theory," Phys. Rev. C **87**, 014006 (2013).

[46] I. Angeli and K.P. Marinova, "Table of experimental nuclear ground state charge radii: An update," At. Data Nucl. Data Tables **99**, 69 – 95 (2013).

[47] N. Schunk, private communication.

[48] J. Simonis, S. Bacca, and G. Hagen, "First principles electromagnetic responses in medium-mass nuclei," (2019), arXiv:1905.02055 [nucl-th].

[49] R. H. Helm, "Inelastic and elastic scattering of 187-mev electrons from selected even-even nuclei," Phys. Rev. **104**, 1466–1475 (1956).

[50] G. Hagen, A. Ekström, C. Forssén, G. R. Jansen, W. Nazarewicz, T. Papenbrock, K. A. Wendt, S. Bacca, N. Barnea, B. Carlsson, C. Drischler, K. Hebeler, M. Hjorth-Jensen, M. Miorelli, G. Orlandini, A. Schwenk, and J. Simonis, "Neutron and weak-charge distributions of the ^{48}Ca nucleus," Nature Physics **12**, 186 (2016).

[51] D.A. Sierra, J. Liao, and D. J. Marfatia, "Impact of form factor uncertainties on interpretations of coherent elastic neutrino-nucleus scattering data," Journal of High Energ. Phys. **141** (2019), https://doi.org/10.1007/JHEP06(2019)141.